Radiology

ORIGINAL RESEARCH • PEDIATRIC IMAGING

MRI and Molecular Characterization of Pediatric High-Grade Midline Thalamic Gliomas: The HERBY Phase II Trial

Daniel Rodriguez, PhD • Raphael Calmon, PhD • Esther Sanchez Aliaga, MD • Daniel Warren, FRCR • Monika Warmuth-Metz, MD • Chris Jones, PhD • Alan Mackay, BSc • Pascale Varlet, PhD • Marie-Cécile Le Deley, PhD • Darren Hargrave, MD • Adela Cañete, MD • Maura Massimino, MD • Amedeo A. Azizi, PhD • Frank Saran, MD • Gudrun Zahlmann, PhD • Josep Garcia, PhD • Gilles Vassal, PhD • Jacques Grill, PhD • Andrew Peet, PhD • Robert A. Dineen, PhD • Paul S. Morgan, PhD • Timothy Jaspan, FRCR

From the Department of Medical Physics and Clinical Engineering (D.R., P.S.M.) and Department of Radiology (R.A.D., T.J.), Nottingham University Hospitals Trust, Derby Rd, Nottingham NG7 2UH, England; Mental Health & Clinical Neurosciences Unit, University of Nottingham, Nottingham, England (D.R., R.A.D., P.S.M.); Department of Pediatric Radiology, Necker Enfants Malades Hospital, Assistance Publique-Hôpitaux de Paris, Paris, France (R.C.); Department of Radiology & Nuclear Medicine, VU University Medical Center, Amsterdam, the Netherlands (E.S.A.); Department of Radiology, Leeds Teaching Hospitals, Leeds, England (D.W.); Institute for Diagnostic and Interventional Neuroradiology, Würzburg University, Würzburg, Germany (M.W.M.); Divisions of Molecular Pathology and Cancer Therapeutics, The Institute of Cancer Research, London, England (C.J., A.M.); Department of Pathological Anatomy and Cytology, Centre Hospitalier Sainte Anne, Paris, France (P.V.); Department of Biostatistics, Centre Oscar Lambret, Lille, France (M.C.L.D.); Department of Haematology and Oncology, Great Ormond Street Hospital, London, England (D.H.); Pediatric Oncology and Hematology Unit, Hospital La Fe, Valencia, Spain (A.C.); Pediatric Oncology Unit, Fondazione IRCCS Istituto Nazionale dei Tumori, Milan, Italy (M.M.); Division of Neonatology, Pediatric Intensive Care and Neuropediatrics, Medical University of Vienna, Vienna, Austria (A.A.A.); Auckland Radiation Oncology, Auckland City Hospital, New Zealand. (F.S.); F. Hoffmann-La Roche, Basel, Switzerland (G.Z., J. Garcia); Department of Pediatric and Adolescent Oncology and Unit 981 from the Institut National de la Santé et de la Recherche Médicale, Gustave Roussy, Université Paris-Saclay, Université Paris-Sud, Villejuif, France (G.V., J. Grill); and Institute of Cancer and Genomic Sciences, University of Birmingham, and Birmingham Children's Hospital, Birmingham, England (A.P.). Received June 26, 2021; revision requested September 9; revision received November 5; accepted February 7, 2022. **Address correspondence to** D.R. (e-mail: *daniel.rodriguez@nuh.nhs.uk*).

Supported by F. Hoffman-La Roche (study number B025041; ClinicalTrials.gov identifier NCT01390948).

Conflicts of interest are listed at the end of this article.

See also the editorial by Widjaja in this issue.

Radiology 2022; 000:1–9 • https://doi.org/10.1148/radiol.211464 • Content codes: NR PD MR

Background: Diffuse midline gliomas (DMG) are characterized by a high incidence of *H3 K27* mutations and poorer outcome. The HERBY trial has provided one of the largest cohorts of pediatric DMGs with available radiologic, histologic-genotypic, and survival data.

Purpose: To define MRI and molecular characteristics of DMG.

Materials and Methods: This study is a secondary analysis of a prospective trial (HERBY; ClinicalTrials.gov identifier, NCT01390948) undertaken between October 2011 and February 2016. Among 121 HERBY participants, 50 had midline nonpontine-based tumors. Midline high-grade gliomas were reclassified into DMG *H3 K27* mutant, *H3* wild type with enhancer of zest homologs inhibitory protein overexpression, epidermal growth factor receptor mutant, or not otherwise stated. The epicenter of each tumor and other radiologic characteristics were ascertained from MRI and correlated with the new subtype classification, histopathologic characteristics, surgical extent, and outcome parameters. Kaplan-Meier curves and log-rank tests were applied to determine and describe survival differences between groups.

Results: There were 42 participants (mean age, 12 years ± 4 [SD]; 23 girls) with radiologically evaluable thalamic-based DMG. Eighteen had partial thalamic involvement (12 thalamopulvinar, six anteromedial), 10 involved a whole thalamus, nine had unithalamic tumors with diffuse contiguous extension, and five had bithalamic tumors (two symmetric, three partial). Twenty-eight participants had DMG *H3 K27* mutant tumors; there were no differences in outcome compared with other DMGs ($n = 4$). Participants who underwent major debulking or total or near-total resection had longer overall survival (OS): 18.5 months vs 11.4 months ($P = .02$). Enrolled participants who developed leptomeningeal metastatic dissemination before starting treatment had worse outcomes (event-free survival, 2.9 months vs 8.0 months [$P = .02$]; OS, 11.4 months vs 18.5 months [$P = .004$]).

Conclusion: Thalamic involvement of diffuse midline gliomas ranged from localized partial thalamic to holo- or bithalamic with diffuse contiguous spread and had poor outcomes, irrespective of *H3 K27* subtype alterations. Leptomeningeal dissemination and less than 50% surgical resection were adverse risk factors for survival.

Clinical trial registration no. NCT01390948

Online supplemental material is available for this article.

Pediatric high-grade gliomas (HGGs) are tumors associated with poor overall survival (1,2). Since the recognition of the new tumoral type of diffuse midline gliomas (DMGs) *H3 K27* mutant in the 2016 World Health Organization classification, four subtypes of DMG have been defined: DMG *H3.3* mutant, DMG *H3.1* mutant, DMG *H3* wild type with enhancer of zest homologs inhibitory protein (*EZHIP*) overexpression, and DMG epidermal growth factor receptor (*EGFR*) mutant (3–5). The subtyping of *H3 K27* mutants is justified by common biologic characteristics based on associated mutations and transcriptomic and methylation profiling (6). This has led to a better understanding of the biologic characteristics and treatment options for patients with these tumors, which

Abbreviations

ADC = apparent diffusion coefficient, DMG = diffuse midline glioma, EFS = event-free survival, *EGFR* = epidermal growth factor receptor, EOR = extent of resection, *EZHIP* = enhancer of zest homologs inhibitory protein, HGG = high-grade glioma, LMM = leptomeningeal metastatic, OS = overall survival, T/NTR = total or near-total resection

Summary

Shorter survival was associated with leptomeningeal metastatic dissemination and lower surgical resection rates irrespective of tumor location and mutational status in participants with thalamic high-grade gliomas in the HERBY trial.

Key Results

- Sixty-nine percent of participants (29 of 42) with midline thalamic high-grade gliomas in the HERBY trial had well-defined tumors with minor or no perilesional edema.
- Tumor location, enhancement pattern, intratumoral diffusion restriction (from MRI), and mutational status did not significantly affect participant survival.
- Leptomeningeal metastatic dissemination, occurring in 42% of participants (16 of 38), was associated with poorer outcomes (event-free survival, 2.9 months vs 8.0 months [$P = .02$]; overall survival, 11.4 months vs 18.5 months [$P = .004$]).

present specific surgical challenges due to their deep anatomic position and eloquent location (7–9). Gliomas symmetrically involving the thalami (bithalamic gliomas) represent a separate subclassification of pediatric midline tumors, molecularly characterized by a high frequency of *EGRF* and/or other mutations in the *EGFR* gene carrying a differentially poorer outcome (3–5,10,11). In contrast, unilateral thalamic tumors lack *EGFR* mutations and have a high frequency of *H3 K27* mutations.

A recent study by Chiba et al (12) evaluated whether any particular anatomic localization within the thalamus was associated with a worse outcome following surgery and correlated this with mutation status and progression or dissemination rate. Ten patients were included in the study, of whom three had low-grade (World Health Organization grade I or II) tumors with no recurrence following surgery and seven had high-grade tumors and a mean overall survival (OS) of 28 months. The authors concluded that there was a distinct biologic tumor profile especially pertaining to the pulvinar that affected prognosis.

The HERBY trial was a randomized, parallel group, multicenter, open-label trial designed to evaluate the addition of bevacizumab to radiation therapy plus temozolomide in pediatric participants with newly diagnosed HGG (13). The correlation of the radiologic imaging with pathologic and molecular analyses for the overall HERBY trial has been recently published (14–16). In this study, we aimed to describe the MRI patterns in this large cohort by using DMG subtypes with higher granularity regarding their molecular characteristics, specifically identifying the tumor epicenter where possible and correlating it with pathologic, molecular, and outcome data. Thus, the purpose of this study was to define MRI and molecular characteristics of DMG.

Materials and Methods

This study is a secondary analysis of the prospective HERBY trial (ClinicalTrials.gov identifier, NCT01390948), which was approved by the applicable independent ethics committees and institutional review boards and conducted in accordance with applicable regulations (International Council for Harmonization of Technical Requirements for Pharmaceuticals for Human Use Good Clinical Practice guidelines and the ethical principles outlined in the Declaration of Helsinki). Written informed consent was obtained from the patient or the parents or legally acceptable representatives before enrollment. Consent was obtained before collection of tissue for the exploratory biomarker analyses. Study accrual occurred between October 2011 and February 2016.

A radiologic analysis of the overall HERBY cohort ($n = 121$) has been published (14). Our study presents a more detailed tumor location analysis for midline HGGs and uses an updated molecular classification. A total of 50 participants were identified who had HGG in a nonpontine midline location, of which 45 had a thalamic or perithalamic epicenter. Three children presenting with a cerebellar tumor (one of whom had an *H3 K27* mutation), one child with a midbrain tegmental tumor, and one child with an anterior third ventricular tumor were excluded. Following post hoc analysis, the tumors of three participants were determined to be low-grade tumors, leaving 42 participants with DMG in the study cohort (Fig 1).

Location

MRI data for the HERBY trial were acquired in accordance with a standardized protocol, which can be accessed in the supplementary materials section of the article by Jaspan et al (17). Preoperative imaging was available in 40 of 42 participants (in two participants, the anatomic location of the tumor site was obtained from study documentation and derived from the postoperative imaging examination). The neuroradiologic assessment was performed by two pediatric neuroradiologists (T.J. and R.A.D., with 34 and 16 years of experience, respectively) in consensus and blinded to outcome. The epicenter of the tumor was determined from an axial T2-weighted or T2-weighted fluid-attenuated inversion-recovery image that best demonstrated the tumor; these two sequences were used because they were universally available for analysis and additional sequences did not provide further useful information to determine site location. Consensus was reached in cases where there was disagreement regarding the tumor epicenter. A precise tumor origin determined with the anatomic localization method described in the study by Chiba et al (12) could not be used because the majority of tumors in the HERBY cohort were large at presentation or could not be categorized into the three groups proposed in their study. Thus, the anatomic epicenter for this study was categorized as *(a)* thalamopulvinar (including thalamopulvinar with capsular extension), *(b)* anteromedial (medial and/or anterior thalamus), *(c)* unilateral whole thalamus, *(d)* whole thalamus with diffuse contiguous spread, or *(e)* bithalamic (including both symmetric and asymmetric tumors) (Fig 1).

Other MRI Features

Details of the MRI analysis methods used for the HERBY trial have been previously described by Rodriguez Gutierrez et al (14). MRI feature characterizations were made with the radiologists blinded to outcome and were recorded as *(a)* tumor margin (well-defined or ill-defined); *(b)* extent of surrounding edema

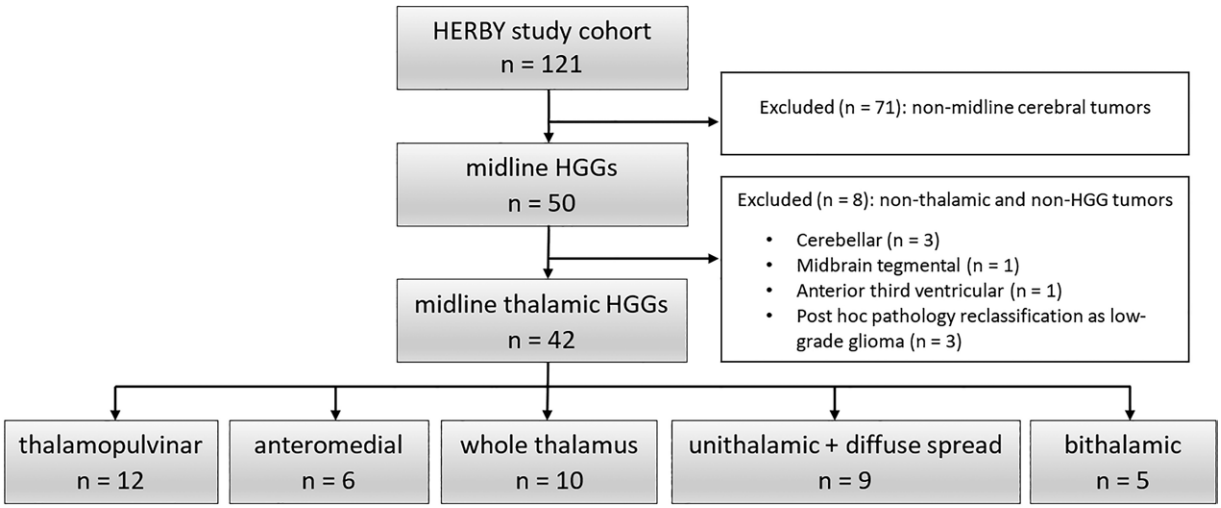

Figure 1: Flowchart shows initial patient cohort of the HERBY trial, exclusion criteria, and final participants with midline thalamic high-grade gliomas (HGGs).

(none, minor, moderate, or severe); *(c)* degree of enhancement (none, minor, moderate, or strong, which was amalgamated into two groups for survival analysis: none or minor and moderate or strong); *(d)* presence or absence of radiologic necrosis (determined as enhancing lesions containing internal irregular areas of low signal intensity, usually having fluid-like characteristics); *(e)* diffusion status (assessed qualitatively as abnormally low apparent diffusion coefficient [ADC] values from diffusion-weighted imaging: restricted diffusion, abnormally high ADC values [ie, increased diffusion], or isointense compared with normal-appearing white matter, as well as quantitatively); and *(f)* presence or absence of leptomeningeal metastatic (LMM) dissemination (identified on two-dimensional T1-weighted and/or three-dimensional T1-weighted contrast-enhanced images).

In addition to these MRI features, the following data were also recorded from the study repository: surgical procedure undertaken; extent of resection (EOR) (total or near-total resection [T/NTR] or major debulking vs minor debulking or biopsy); histologic findings; treatment stratification (radiation therapy and temozolomide or radiation therapy and temozolomide plus bevacizumab); pseudoprogression and pseudoresponse (defined as an increase of contrast enhancement and/or edema at MRI without true tumor progression or a decrease in contrast enhancement without a decrease of tumor activity, respectively); clinical status at the end of the study; event-free survival (EFS); and OS. EFS and OS criteria for the HERBY trial have previously been described by Grill et al (13).

Molecular Analysis

Previous analysis of the HERBY cohort used the World Health Organization 2007 classification that was updated in 2016. This study used the latest cIMPACT-NOW (Consortium to Inform Molecular and Practical Approaches to Central Nervous System Tumor Taxonomy) guidelines (18) and recently published data to differentiate four subtypes of thalamic DMGs (3–5): DMG *H3 K27* mutant (determined with use of sequencing and/or immunostaining); DMG *H3* (wild type) with *EZHIP* overexpression (determined with sequencing and *EZHIP* immunostaining); DMG *EGFR* mutant (determined with sequencing and immunostaining), or DMG not otherwise stated (loss of *H3 K27* me3 trimethylation but no sequencing, methylation class, or other available immunostainings). Not enough material was available for one midline HGG subtyping.

Statistical Analysis

The Fisher exact test was used to test relationships between categorical variables (with use of the Freeman-Halton extension for variables with more than two categories): location, margin definition, enhancement, radiologic necrosis, diffusion restriction, extent of resection, and LMM dissemination. Kruskal-Wallis tests were used for continuous variables (ADC values). Kaplan-Meier curves were used to describe EFS and OS over time, and log-rank tests were applied to determine survival differences between groups according to location, EOR, and the presence of *H3 K27* mutation. $P < .05$ was considered indicative of statistically significant difference, adjusted with use of Bonferroni correction (by multiplying the observed P value by the number of comparisons made) in cases of multiple comparison. All data analysis was conducted using SPSS Statistics for Windows, version 25 (IBM).

Results

Patient Characteristics

Forty-two participants were included, with a mean age of 12 years ± 4 (SD) and a male-to-female ratio of 19 to 23. An overview of the DMG cohort of the HERBY trial is provided in the Table. A comprehensive list for each participant is included in Table E1 (online).

Location Detail

Figure 2 displays examples of the five different anatomic locations defined as having a thalamic epicenter based on T2-weighted imaging. Figure 3 shows the frequencies according to the five defined thalamic anatomic locations; further details about the classification and consensus can be found in Table E1 and Figures E1–E4 (online).

Amalgamated Thalamic Location Groups and Their Demographic, Treatment, Radiologic, Pathologic, and Genomic Mutation Characteristics

Characteristic	Thalamopulvinar (*n* = 12)	Anteromedial (*n* = 6)	Whole Thalamus (*n* = 10)	Unithalamic with Diffuse Spread (*n* = 9)	Bithalamic (*n* = 5)
Age (y)*	13 (9–17)	12 (7–15)	11 (6–18)	11 (4–17)	9 (5–16)
Sex					
F	8	2	6	4	3
M	4	4	4	5	2
EFS (mo)†	4.1 (0.0–21.5)	8.4 (2.3–14.8)	5.5 (0.0–19.8)	6.4 (0.6–11.1)	10.0 (2.6–11.1)
OS (mo)†	11.0 (0.1–24.4)	15.1 (10.6–30.5)	14.4 (0.3–20.8)	8.6 (0.6–17.4)	12.6 (7.9–16.6)
Tumor margin					
Well-defined	11	5	9	1	3
Ill-defined	1	1	1	8	2
Peritumoral edema					
None	9	5	9	6	2
Minor	2	1	0	2	3
Moderate	1	0	0	0	0
Severe	0	0	0	0	0
NA	0	0	1	1	0
Enhancement					
None	0	2	1	3	2
Minor	2	2	4	2	0
Moderate	2	0	1	0	0
Strong	8	1	4	4	3
NA	0	1	0	0	0
Radiologic necrosis					
Present	11	1	8	4	3
Absent	0	4	2	5	2
NA	1	1	0	0	0
Diffusion					
Increased	2	5	2	4	3
Restricted	5	0	7	3	2
NA	5	1	1	2	0
Surgical resection					
Total or NTR	6	1	4	0	0
Major debulking	4	0	1	0	1
Minor debulking	1	2	3	2	0
Biopsy	1	3	2	7	4
Treatment arm					
RT + TMZ	5	3	5	5	2
Bev	6	3	5	4	2
NA	1	0	0	0	1
LMM dissemination					
Yes	6	2	2	4	2
No	5	4	8	3	2
NA	1	0	0	2	1
Pseudoprogression					
Yes	0	0	1	0	0
No	11	6	8	7	4
NA	1	0	1	2	1
WHO grade					
Grade III	0	5	4	5	2
Grade IV	12	1	6	4	3
Molecular alterations					
DMG, *H3 K27* m	10	5	8	4	1

(Table *continues*)

***(continued)* Amalgamated Thalamic Location Groups and Their Demographic, Treatment, Radiologic, Pathologic, and Genomic Mutation Characteristics**

Characteristic	Thalamopulvinar (n = 12)	Anteromedial (n = 6)	Whole Thalamus (n = 10)	Unithalamic with Diffuse Spread (n = 9)	Bithalamic (n = 5)
DMG, wild type *EZHIP* oe	0	0	0	2	0
DMG, *EGFR*m	0	0	0	1	1
DMG NOS	2	0	2	2	3
NA	0	1	0	0	0

Note.—Unless otherwise specified, data are numbers of participants. Bev = radiation therapy plus temozolomide plus bevacizumab, DMG = diffuse midline glioma, EFS = event-free survival, *EGFR* = epidermal growth factor receptor, *EZHIP* = enhancer of zest homologs inhibitory protein, LMM = leptomeningeal metastatic, m = mutant, NA = not available, NOS = not otherwise stated, NTR = near-total resection, oe = overexpression, OS = overall survival, RT + TMZ = radiation therapy plus temozolomide, WHO = World Health Organization.

* Data are means, with ranges in parentheses.

† Data are medians, with ranges in parentheses.

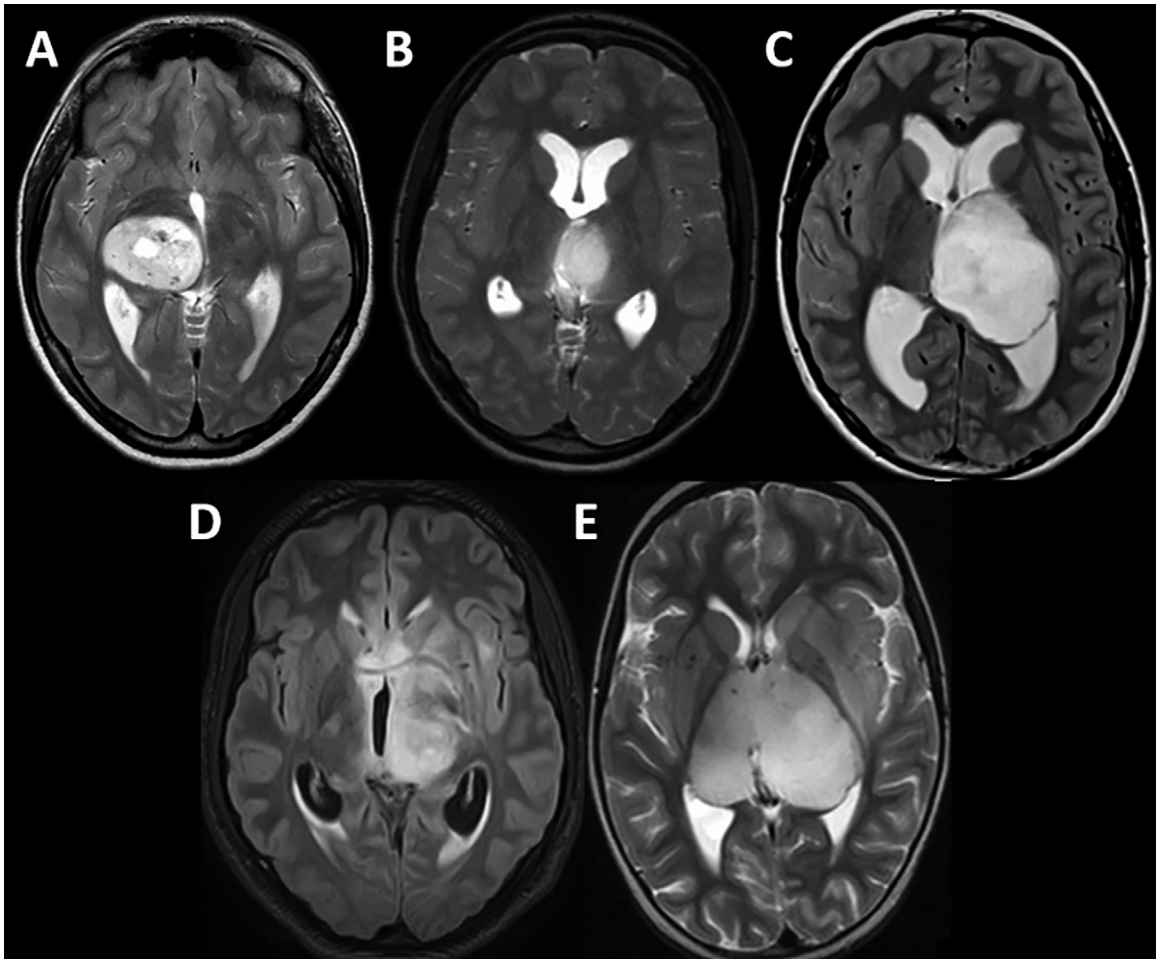

Figure 2: Classification of thalamic-based gliomas with exemplar imaging of the five anatomic locations. Axial T2-weighted images at the level of the tumor isocenter show **(A)** thalamopulvinar tumor in a 14-year-old girl, **(B)** anteromedial tumor in a 10-year-old boy, **(C)** whole-thalamus tumor in a 12-year-old boy, **(D)** unithalamic tumor with diffuse contiguous spread into the adjacent capsular and anterior striatal region in a 15-year-old girl, and **(E)** bithalamic tumor in a 17-year-old girl, with involvement of the posterior putamen and insular cortex on the left.

Tumor Margin Definition and Peritumoral Edema

Most midline tumors (29 of 42, 69%) were radiologically well-defined. Tumor margin definition was different across thalamic location, with ill-defined tumors (n = 13) occurring mostly in unithalamic tumors with diffuse contiguous spread (eight of nine) and bithalamic tumors (two of five) ($P < .001$).

Perilesional edema was absent or minor in 98% of participants (39 of 40), with moderate edema in one participant. In

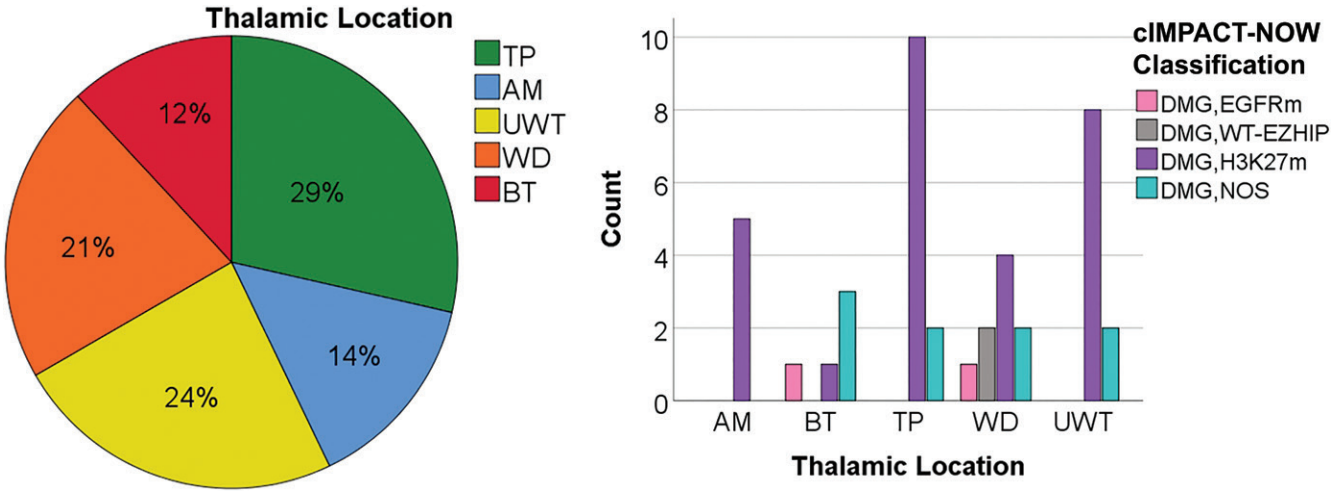

Figure 3: Left: Pie chart shows percentages for each anatomic location of the thalamic diffuse midline gliomas (DMGs) in the HERBY cohort (*n* = 42): unilateral thalamopulvinar, including capsular extension (TP); anteromedial and medial thalamus (AM); unilateral whole thalamus, with no spread (UWT); thalamic, with diffuse adjacent spread (WD); and bithalamic (BT). Right: Bar graph shows molecular alterations across the same locations (*n* = 41; one sample had insufficient material for analysis). cIMPACT-NOW = Consortium to Inform Molecular and Practical Approaches to Central Nervous System Tumor Taxonomy, EGFRm = epidermal growth factor receptor mutant, H3K27m = *H3 K27* mutant, NOS = not otherwise stated, WT-EZHIP = wild-type enhancer of zest homologs inhibitory protein.

the two participants in whom preoperative imaging was not available, postoperative scans showed no edema around the margins of the resected tumor.

Tumor Enhancement Pattern and Radiologic Necrosis

While thalamopulvinar tumors showed the greatest proportion of moderate or strong enhancement (10 of 12), with a more varied and heterogeneous pattern of enhancement in the other four groups, we found no evidence that tumor enhancement patterns differed across thalamic location ($P = .20$).

Intratumoral necrosis (as defined at MRI) was seen in 27 participants, absent in 13, and could not be determined in two. The incidence of intratumoral necrosis differed across thalamic locations ($P = .008$). Intratumoral necrosis was observed in all thalamopulvinar tumors ($n = 11$) and in one of five anteromedial tumors, eight of 10 whole thalamic tumors, four of nine unithalamic tumors with diffuse spread, and three of five bithalamic tumors.

Diffusion Characteristics

Although we found no evidence of group differences in regard to areas of restricted diffusion across thalamic location ($P = .05$), most tumors showing diffusion restriction were in the whole thalamus (seven of nine), thalamopulvinar (five of seven), and thalamic tumors with diffuse contiguous spread (four of seven) groups. A quantitative analysis of minimum ADC values showed a similar pattern of lower ADC values in the same groups ($P = .34$) (Fig E1 [online]).

Surgical Resection

The extent of surgical resection differed across thalamic location, being greatest (either major debulking or T/NTR) in the thalamopulvinar group (10 of 12 tumors), intermediate in the whole thalamic group (six of 10 tumors), and least in the bithalamic (one of five tumors) and unithalamic with diffuse contiguous spread (zero of nine tumors) groups, where 11 of the 14 had biopsies only ($P < .001$).

LMM Dissemination

LMM disease, developing after study entry but before commencement of treatment, was present in 16 of 38 of the evaluable participants (42%). Four participants died soon after study entry and therefore could not be evaluated regarding LMM status. The location of the LMM dissemination was infratentorial in three participants (two of them with no spinal imaging), infra- and supratentorial in four participants (three of them with no spinal imaging), only spinal in five participants, and spinal and intracranial in four participants. There was no evidence that LMM dissemination differed across thalamic locations ($P = .46$).

Pseudoprogression or Pseudoresponse

Only one participant, who had a unilateral whole thalamic tumor, manifested imaging evidence of pseudoprogression. Pseudoresponse was not identified in the study cohort.

Histologic and Molecular Findings

Molecular studies were available for all participants with DMG except one (not enough material to determine the loss of *H3 K27* trimethylation). In the nine participants with DMG not otherwise stated, tumors were classified as DMG based on the loss of *H3 K27* me3 trimethylation, but it was not possible to differentiate between the three different subtypes. The remaining tumors were DMG *H3 K27* mutant ($n = 28$); DMG *H3* wild type with *EZHIP* overexpression ($n = 2$); and DMG *EGFR* mutant ($n = 2$).

Across location groups, DMGs were classified as the DMG *H3 K27* mutant subtype in 10 of 12 thalamopulvinar, five of six anteromedial, eight of 10 unithalamic whole thalamus, four of nine thalamic with contiguous spread, and one of five of bithalamic tumors. There was no evidence that the frequency of *H3 K27* mutation differed across thalamic location ($P = .05$).

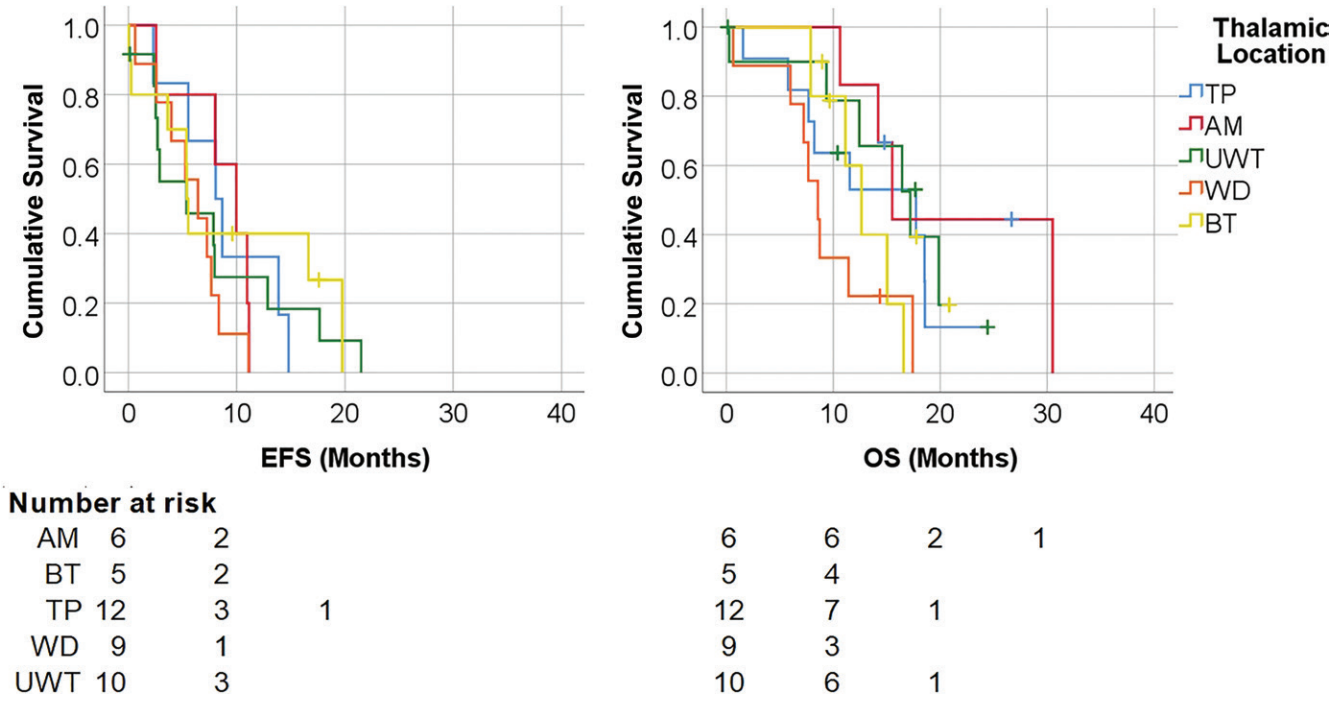

Figure 4: Survival curves show event-free survival (EFS) and overall survival (OS) of participants with thalamic diffuse midline glioma in the HERBY trial (n = 42). The anatomic locations are unilateral thalamopulvinar, including capsular extension (TP); anteromedial and medial thalamus (AM); unilateral whole thalamus, with no spread (UWT); thalamic, with diffuse adjacent spread (WD); and bithalamic (BT). There were no significant differences in survival between these groups (median EFS = 4.1, 8.4, 5.5, 6.4, and 10.0 months, respectively [log-rank P = .97], and median OS = 11.0, 15.1, 14.4, 8.6, and 12.6 months [P = .62]).

Outcome Parameters

We found no evidence of differences in survival across the location groups (log-rank P = .97 for EFS and P = .62 for OS). See Figure 4 for the survival curves.

Tumor enhancement patterns showed no influence on outcome between the 23 participants (one had no preoperative MRI examination for evaluation) with tumors showing moderate or strong enhancement (median EFS, 5.5 months; median OS, 14.4 months) compared with the 18 participants with mild or no enhancement (median EFS, 7.8 months; median OS, 11.5 months) (log-rank P = .59 for EFS and P = .27 for OS).

We found no difference in OS between participants with tumors exhibiting areas of restricted diffusion (median EFS, 5.4 months; median OS, 11.1 months) and those with tumors showing homogeneously increased diffusion (median EFS, 8.4 months; median OS, 15.5 months) (log-rank P = .07 for EFS and P = .09 for OS).

We found no differences in EFS regarding the extent of surgical resection: biopsy, minor debulking, major debulking, and T/NTR had a median EFS of 7.7, 5.3, 5.4, and 7.9 months, respectively (log-rank P = .14), but there were differences in median OS (11.3, 10.6, 17.7, and 18.5 months, respectively; log-rank P = .01) (Fig E2 [online]). Participants with more than 50% resection (major debulking or T/NTR) had longer OS (18.5 months vs 11.4 months; log rank P = .02) (Fig E3 [online]).

Participants with DMG *H3 K27* mutant (n = 28) had a median EFS of 5.5 months and a median OS of 16.4 months. The two participants with DMG *H3* wild type with *EZHIP* overexpression had a mean EFS of 5.5 months and a mean OS of 14.4 months. The two participants with DMG *EGFR* mutant had a mean EFS of 8.6 months and a mean OS of 10.6 months. We found no difference in survival outcomes between participants with thalamopulvinar DMG *H3* K27 mutant (n = 10) and DMG *H3 K27* mutant from other locations (n = 18) (median EFS, 2.7 months vs 8.0 months [log-rank P = .86] and median OS, 14.8 months vs 8.2 months [log-rank P = .61]) (Fig E4 [online]).

Participants who developed LMM dissemination had a worse median EFS (2.9 months) and OS (11.4 months) than those who did not (median EFS, 8.0 months; median OS, 18.5 months [log-rank P = .02 for EFS and P = .004 for OS]). The poorer outcome in these participants was independent of the volume or the disseminated tumor. In seven participants, LMM dissemination was identified within 3 months of participant enrollment in the study.

Discussion

Following the 2016 World Health Organization reclassification of pediatric midline high-grade glioma (HGG), we performed a post hoc analysis of a large cohort of participants with midline tumors extracted from the HERBY trial data to provide a risk stratification of these tumors, focusing on localization, imaging characterization, and correlation with molecular findings. Five anatomic subtypes of thalamic-centric HGG are described; 28 participants had tumors confined to the thalamus, with partial involvement in 18 (anteromedial, n = 6; thalamopulvinar, n = 12) and involvement of the whole thalamus in 10. Fourteen participants had diffuse contiguous tumor spread associated with a unithalamic tumor (n = 9) or bithalamic tumor (n = 5). Factors

that carried significantly adverse survival risk were *(a)* subtotal or minimal tumor resection or biopsy (overall survival [OS], 18.5 months vs 11.4 months [P = .02]) and leptomeningeal metastatic dissemination after study entry (event-free survival, 2.9 months vs 8.0 months [P = .02]; OS, 11.4 months vs 18.5 months [P = .004]).

A recent study by Chiba et al (12) radiologically classified thalamic gliomas based on 10 patients and suggested a risk stratification; however, only seven were HGGs, and genotyping was incomplete. A new classification of DMGs derived from the larger cohort of the HERBY trial shows different patterns of thalamic involvement with distinct radiologic features and EOR. The results from HERBY can be compared with those from a recent retrospective histopathologic review of pediatric patients with nonpontine DMGs from the German HIT-HGG registry (19), coupled with identification of the *H3* mutational status. Among 85 children aged 3–18 years, 32 had a thalamic tumor, with 24 of those tumors harboring an *H3 K27* mutation and eight *H3* wild-type tumors. No survival benefit was conferred by anatomic location, and—unlike in HERBY—there was no survival benefit according to EOR. In their study, patients with *H3 K27M* tumors did have a shorter survival than those with other non–*H3 K27M* DMGs, but non–*H3 K27M* DMG numbers in HERBY were too few to compare. In contrast to the study by Chiba et al, HERBY participants with thalamopulvinar tumors with *H3 K27* mutations did not appear to have different survival outcomes compared with participants with other thalamic DMGs.

Most midline tumors in the HERBY cohort were large at outset, involving most or all of the thalamus, which made determining tumor origin within the thalamus impossible. Consequently, a new anatomic classification was used, also accounting for bilateral thalamic tumors and tumors involving a whole thalamus with diffuse contiguous spread. The reason for the lower incidence of partial thalamic tumors in our study is uncertain; all patients in the Chiba cohort underwent tumor resection and were analyzed retrospectively; this may have led to selection bias toward more resectable tumors. Our study includes a higher proportion of holothalamic or bithalamic tumors, likely reflecting a truer representation of all thalamic HGGs at presentation.

The majority (69%, 29 of 42) of the HERBY DMGs were radiologically well-defined, with little or no peritumoral edema (98%, 39 of 40) (unlike their cerebral counterparts); were mostly *H3 K27* mutant subtype (67%, 28 of 42); and presented variable patterns of enhancement and diffusion (51%; diffusion-weighted imaging in the 18 of 35 of participants for whom it was available showed intratumoral diffusion restriction), high incidences of (radiologically defined) necrosis (68%, 27 of 40), and LMM dissemination (42%, 16 of 38). Across the five thalamic locations, there were differences in margin definition, incidence of necrosis, and EOR. Whereas there was no evidence of a difference in EFS according to EOR, there was a difference in OS (participants who underwent major debulking or T/NTR survived longer). There were no differences in survival according to location, tumor enhancement, or diffusion restriction. LMM dissemination resulted in poorer survival outcome.

The role of tumor resection for midline pediatric HGG remains uncertain (20,21), with limited scope for maximal resection of thalamic tumors (22). In a recently published single-center retrospective analysis (49 children <18 years of age with a thalamic tumor presenting between 1992 and 2018; 50% nonpilocytic infiltrative gliomas and 28% tumors with *H3 K27* mutations) (23), EOR, ascertained on the basis of MRI, was stratified between major debulking (>50% tumor resection) in 16 of 25 patients (>90% resection in eight, 50%–90% resection in eight) and biopsy in the remaining nine patients. The authors found a survival benefit for patients undergoing major debulking. The results from the HERBY cohort also found a longer OS for the participants who underwent major debulking, but no differences in EFS.

In the HERBY trial, only five participants had bithalamic tumors. Two showed symmetric thalamic involvement; three had a unilateral thalamic tumor with partial involvement of the contralateral thalamus, with one exhibiting *EGFR* amplification. The only other DMG showing *EGFR* amplification was unithalamic with diffuse contiguous tumor extension.

There are several limitations to our study. The trial was not designed to address the present post hoc analysis; the small number of DMGs precluded multivariable survival analysis, so it is unknown whether the reported findings are independent risk factors. Similarly, the results of the univariable analyses performed can only be considered indicative, as some are clearly underpowered with small patient numbers in each location group. Third, advanced imaging techniques (perfusion-weighted imaging, MR spectroscopy) were only used for a minority of participants and/or were only intermittently undertaken, limiting the possibility of assessing the value of advanced imaging in these tumors. Last, although a consensus was reached for each image, the determination of the tumor location within the thalamus was associated with relatively high uncertainty.

The findings in this study have potentially importance for surgical and radiotherapeutic management of thalamic-based diffuse midline gliomas. Further research is required to assess whether adapting radiation therapy fields to patients with these tumors should be adopted more widely in view of their poor prognostic outcome. The results from the HERBY trial have recently been incorporated into the Response Assessment of Pediatric Neuro-Oncology, or RAPNO, guidelines for pediatric high-grade glioma (22). Adopting the principles and protocols addressed in these guidelines may help with the design and utility of future pediatric tumor studies.

Acknowledgments: We acknowledge the help and support for this research from the following bodies: the Australian Children's Cancer Trust (ACCT), Innovative Therapies for Children with Cancer (ITCC), and European Society for Paediatric Oncology (SIOPE). All research at Great Ormond Street Hospital NHS Foundation Trust and UCL Great Ormond Street Institute of Child Health is made possible by the UK NIHR Great Ormond Street Hospital Biomedical Research Centre. NHS funding to the National Institute for Health Research Biomedical Research Centre at The Royal Marsden and the ICR. P.S.M. and R.A.D. are members of the UK National Institute of Health Research's Nottingham Biomedical Research Centre. The views expressed are those of the author(s) and not necessarily those of the NHS, the NIHR, or the Department of Health.

Author contributions: Guarantors of integrity of entire study, **D.R., P.S.M., T.J.**; study concepts/study design or data acquisition or data analysis/interpretation, all authors; manuscript drafting or manuscript revision for important intellectual content, all authors; approval of final version of submitted manuscript, all authors; agrees to ensure any questions related to the work are appropriately resolved, all

authors; literature research, **D.R., F.S., G.Z., T.J.**; clinical studies, **D.W., M.W.M., D.H., M.M., A.A.A., G.Z., J. Garcia, G.V., J. Grill, A.P., T.J.**; experimental studies, **D.R., C.J., P.S.M., T.J.**; statistical analysis, **D.R., C.J., A.M.**; and manuscript editing, **D.R., R.C., E.S.A., D.W., M.W.M., D.H., A.C., M.M., F.S., G.Z., R.A.D., P.S.M., T.J.**

Data sharing: All data generated or analyzed during the study are included in the published paper.

Disclosures of conflicts of interest: D.R. No relevant relationships. **R.C.** No relevant relationships. **E.S.A.** No relevant relationships. **D.W.** No relevant relationships. **M.W.M.** No relevant relationships. **C.J.** No relevant relationships. **A.M.** No relevant relationships. **P.V.** No relevant relationships. **M.C.L.D.** No relevant relationships. **D.H.** No relevant relationships. **A.C.** Consulting fees from Eusa Pharma and Y-mAbs Therapeutics; support for attending meetings and/or travel from Eusa Pharma; member of the data monitoring committee for EU Clinical Trials Register no. NB2015-LR; vice president of SEHOP. **M.M.** Consulting fees from Roche; support for attending meetings and/or travel from Roche. **A.A.A.** No relevant relationships. **F.S.** Personal fees from Roche. **G.Z.** Stock or stock options in F. Hoffman-La Roche. **J. Garcia** No relevant relationships. **G.V.** Support for attending meetings from F. Hoffman-La Roche. **J. Grill** Support for attending meetings and/or travel from F. Hoffman-La Roche and Genentech. **A.P.** National Institute of Health Research (NIHR) Research Professorship NIHR-RP-R2-12-019. **R.A.D.** Research grants to institution from the NIHR, Action for A-T Project, and Children's Cancer and Leukaemia Group; chair of the Academic Sub-Committee of the British Society of Neuroradiologists. **P.S.M.** Co-chair of the European Society for Paediatric Oncology Brain Tumour Imaging Group. **T.J.** No relevant relationships.

References

1. Jones C, Karajannis MA, Jones DTW, et al. Pediatric high-grade glioma: biologically and clinically in need of new thinking. Neuro Oncol 2017;19(2):153–161.
2. Sturm D, Pfister SM, Jones DTW. Pediatric gliomas: current concepts on diagnosis, biology, and clinical management. J Clin Oncol 2017;35(21):2370–2377.
3. Castel D, Philippe C, Calmon R, et al. Histone H3F3A and HIST1H3B K27M mutations define two subgroups of diffuse intrinsic pontine gliomas with different prognosis and phenotypes. Acta Neuropathol (Berl) 2015;130(6):815–827.
4. Castel D, Kergrohen T, Tauziède-Espariat A, et al. Histone H3 wild-type DIPG/DMG overexpressing EZHIP extend the spectrum diffuse midline gliomas with PRC2 inhibition beyond H3-K27M mutation. Acta Neuropathol (Berl) 2020;139(6):1109–1113.
5. Sievers P, Sill M, Schrimpf D, et al. A subset of pediatric-type thalamic gliomas share a distinct DNA methylation profile, H3K27me3 loss and frequent alteration of EGFR. Neuro Oncol 2021;23(1):34–43.
6. Castel D, Philippe C, Kergrohen T, et al. Transcriptomic and epigenetic profiling of 'diffuse midline gliomas, H3 K27M-mutant' discriminate two subgroups based on the type of histone H3 mutated and not supratentorial or infratentorial location. Acta Neuropathol Commun 2018;6(1):117.
7. Wu G, Broniscer A, McEachron TA, et al. Somatic histone H3 alterations in pediatric diffuse intrinsic pontine gliomas and non-brainstem glioblastomas. Nat Genet 2012;44(3):251–253.
8. Aihara K, Mukasa A, Gotoh K, et al. H3F3A K27M mutations in thalamic gliomas from young adult patients. Neuro Oncol 2014;16(1):140–146.
9. Solomon DA, Wood MD, Tihan T, et al. Diffuse midline gliomas with histone H3-K27M mutation: a series of 47 cases assessing the spectrum of morphologic variation and associated genetic alterations. Brain Pathol 2016;26(5):569–580.
10. Mondal G, Lee JC, Ravindranathan A, et al. Pediatric bithalamic gliomas have a distinct epigenetic signature and frequent EGFR exon 20 insertions resulting in potential sensitivity to targeted kinase inhibition. Acta Neuropathol (Berl) 2020;139(6):1071–1088.
11. Reardon DA, Gajjar A, Sanford RA, et al. Bithalamic involvement predicts poor outcome among children with thalamic glial tumors. Pediatr Neurosurg 1998;29(1):29–35.
12. Chiba K, Aihara Y, Masui K, Abe K, Komori T, Kawamata T. Pulvinar locus is highly relevant to patients' outcomes in surgically resected thalamic gliomas in children. World Neurosurg 2020;134:e530–e539.
13. Grill J, Massimino M, Bouffet E, et al. Phase II, open-label, randomized, multicenter trial (HERBY) of bevacizumab in pediatric patients with newly diagnosed high-grade glioma. J Clin Oncol 2018;36(10):951–958.
14. Rodriguez Gutierrez D, Jones C, Varlet P, et al. Radiological evaluation of newly diagnosed non-brainstem pediatric high-grade glioma in the HERBY phase II trial. Clin Cancer Res 2020;26(8):1856–1865.
15. Mackay A, Burford A, Molinari V, et al. Molecular, pathological, radiological, and immune profiling of non-brainstem pediatric high-grade glioma from the HERBY phase II randomized trial. Cancer Cell 2018;33(5):829–842.e5.
16. Varlet P, Le Teuff G, Le Deley MC, et al. WHO grade has no prognostic value in the pediatric high-grade glioma included in the HERBY trial. Neuro Oncol 2020;22(1):116–127.
17. Jaspan T, Morgan PS, Warmuth-Metz M, et al. Response assessment in pediatric neuro-oncology: implementation and expansion of the RANO criteria in a randomized phase II trial of pediatric patients with newly diagnosed high-grade gliomas. AJNR Am J Neuroradiol 2016;37(9):1581–1587.
18. Louis DN, Aldape K, Brat DJ, et al. Announcing cIMPACT-NOW: the Consortium to Inform Molecular and Practical Approaches to CNS Tumor Taxonomy. Acta Neuropathol 2017;133(1):1–3.
19. Karremann M, Gielen GH, Hoffmann M, et al. Diffuse high-grade gliomas with H3 K27M mutations carry a dismal prognosis independent of tumor location. Neuro Oncol 2018;20(1):123–131.
20. Baroncini M, Vinchon M, Minéo JF, Pichon F, Francke JP, Dhellemmes P. Surgical resection of thalamic tumors in children: approaches and clinical results. Childs Nerv Syst 2007;23(7):753–760.
21. Kramm CM, Butenhoff S, Rausche U, et al. Thalamic high-grade gliomas in children: a distinct clinical subset? Neuro Oncol 2011;13(6):680–689.
22. Erker C, Tamrazi B, Poussaint TY, et al. Response assessment in paediatric high-grade glioma: recommendations from the Response Assessment in Pediatric Neuro-Oncology (RAPNO) working group. Lancet Oncol 2020;21(6):e317–e329.
23. Dorfer C, Czech T, Gojo J, et al. Infiltrative gliomas of the thalamus in children: the role of surgery in the era of H3 K27M mutant midline gliomas. Acta Neurochir (Wien) 2021;163(7):2025–2035.